



An introduction to Fluid-Thermo Dynamics modelling using an open-source CFD software

Dr. Najmeh Foroozani

Computational Studies and Molecular Dynamic Simulations workshop

University of Ibadan, Ibadan

April 2019



- DAY 2 morning

Computational methods for Fluid Dynamics (CFD)



Recall

- Equations of motion for an incompressible flow:

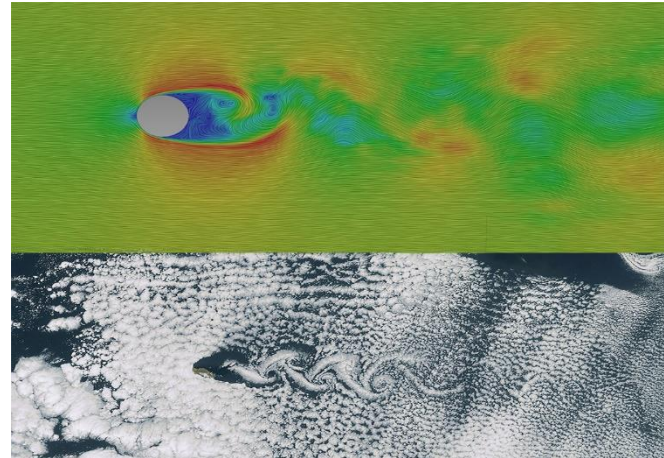
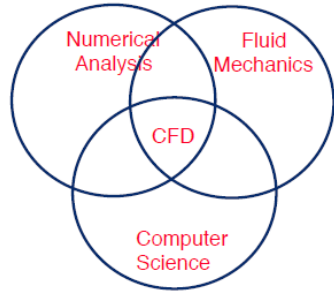
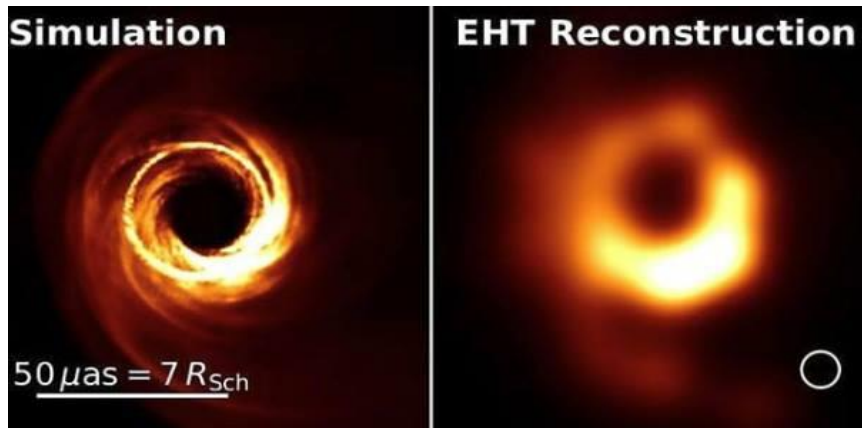
$$\frac{\partial u}{\partial x} + \frac{\partial v}{\partial y} + \frac{\partial w}{\partial z} = 0$$

$$\rho \left(\frac{\partial u}{\partial t} + u \frac{\partial u}{\partial x} + v \frac{\partial u}{\partial y} + w \frac{\partial u}{\partial z} \right) = - \frac{\partial P}{\partial x} + \rho g_x + \mu \left(\frac{\partial^2 u}{\partial x^2} + \frac{\partial^2 u}{\partial y^2} + \frac{\partial^2 u}{\partial z^2} \right)$$

$$\rho \left(\frac{\partial v}{\partial t} + u \frac{\partial v}{\partial x} + v \frac{\partial v}{\partial y} + w \frac{\partial v}{\partial z} \right) = - \frac{\partial P}{\partial y} + \rho g_y + \mu \left(\frac{\partial^2 v}{\partial x^2} + \frac{\partial^2 v}{\partial y^2} + \frac{\partial^2 v}{\partial z^2} \right)$$

$$\rho \left(\frac{\partial w}{\partial t} + u \frac{\partial w}{\partial x} + v \frac{\partial w}{\partial y} + w \frac{\partial w}{\partial z} \right) = - \frac{\partial P}{\partial z} + \rho g_z + \mu \left(\frac{\partial^2 w}{\partial x^2} + \frac{\partial^2 w}{\partial y^2} + \frac{\partial^2 w}{\partial z^2} \right)$$

Simulation or?





What is CFD?

Computational fluid dynamics (CFD):

CFD is the analysis, by means of computer-based simulations, of systems involving fluid flow, heat transfer and associated phenomena such as chemical reactions.

CDF applications

Aerospace

Automobile industry

Engine design and performance

The energy sector

Oil and gas

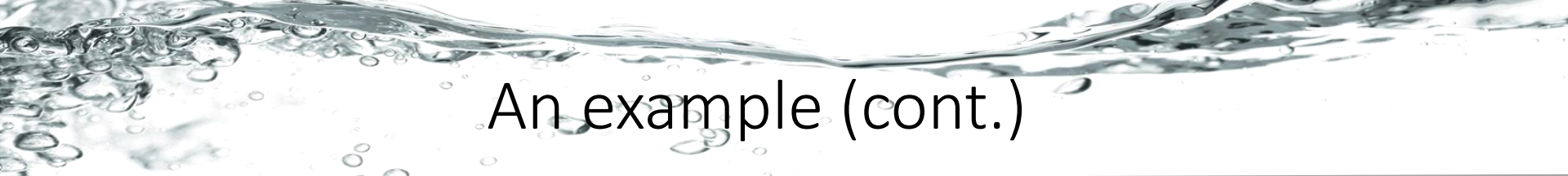
Biofluids

Many other sectors



What does CFD involve?

- Specification of the problem
- Development of the physical model
- Development of the mathematical model
 - Governing equations
 - Boundary conditions
 - Turbulence modelling
- Mesh generation
- Discretization of the governing equations
- Solution of discretized equations
- Post processing
- Interpretation of the results

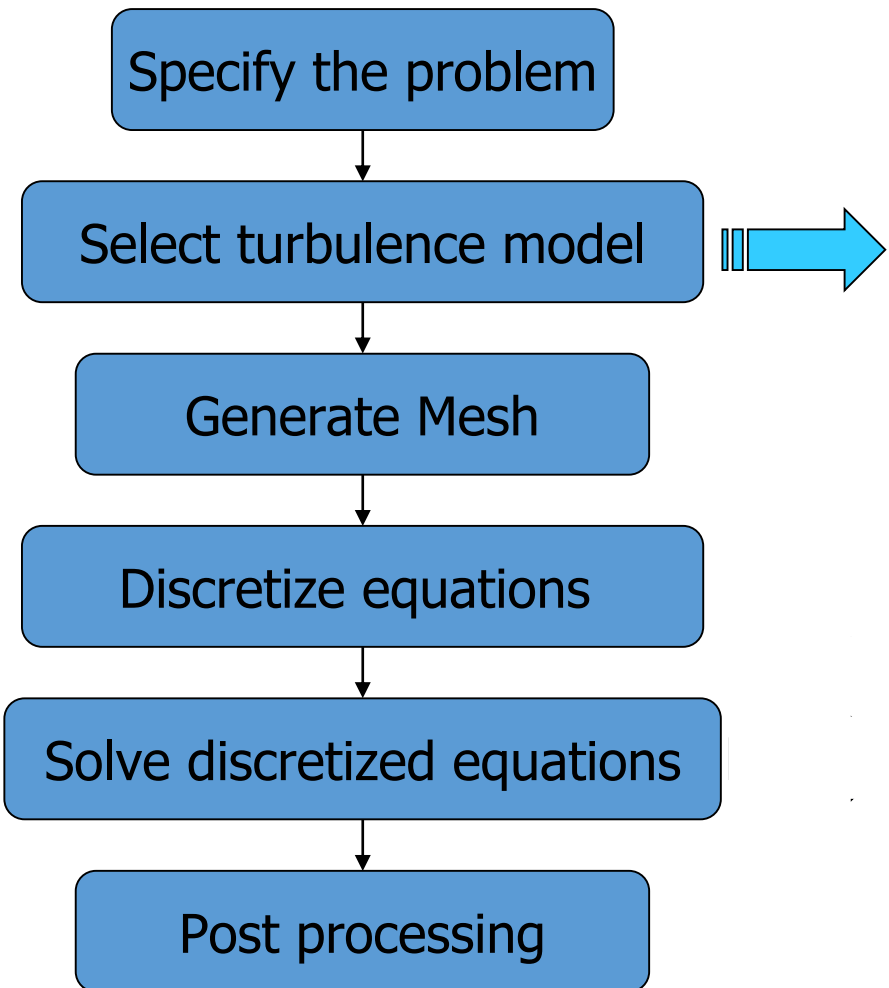


An example (cont.)

Development of the mathematical model

- Governing equations
 - Equations: momentum, thermal (x), multiphase (x), ...
 - Phase 1: 2D, steady; Phase 2: unsteady, ...,
 - The flow is turbulent!
- Boundary conditions
 - Decide the computational domain
 - Specify boundary conditions
- Mesh generation
 - Finer mesh near the wall but not too close to wall
 - Finer mesh behind the pipe

CFD road map



Turbulence models

- These are semi-empirical mathematical models introduced to CFD to describe the turbulence in the flow

Main topics

- Three levels of CFD simulations
- Classification of turbulence models
- Examples of popular models
- Special considerations
- General remarks about turbulence modelling

Finite difference (FD)

Starting from the differential form of the equations

The computational domain is covered by a grid

At each grid point, the differential equations (partial derivatives) are approximated

Only used in structured grids and normally straightforward

Disadvantage: conservation is not always guaranteed

Disadvantage: Restricted to simple geometries.

Finite Volume (FV)

Starting from the integral form of the equations

The solution domain is covered by control volumes (CV)

The conservation equations are applied to each CV

The FV can accommodate any type of grid and suitable for complex geometries

The method is conservative (as long as surface integrals are the same for CVs sharing the boundary) *Most widely used method in CFD*

Disadvantage: more difficult to implement higher than 2nd order methods in 3D.

Finite element (FE)

The domain is broken into a set of discrete volumes: finite elements

The equations are multiplied by a weight function before they are integrated over the entire domain.

The solution is to search a set of non-linear algebraic equations for the computational domain.

Advantage: FE can easily deal with complex geometries.

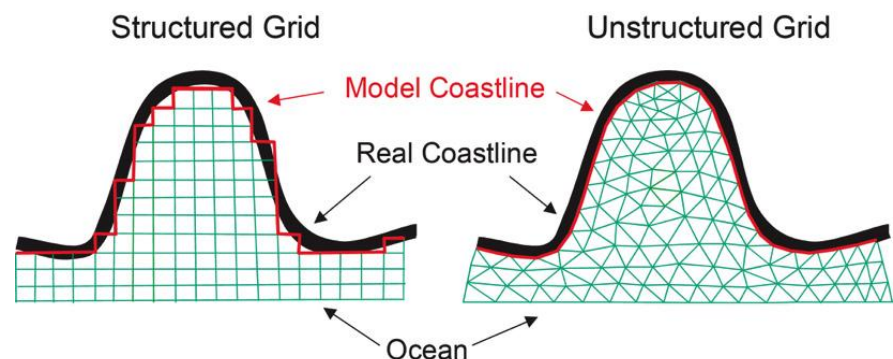
Disadvantage: since unstructured in nature, the resultant matrices of linearized equations are difficult to find efficient solution methods. Not often used in CFD

Geometry

- The starting point for all problems is a “geometry.”
- The geometry describes the shape of the problem to be analyzed.
- Can consist of volumes, faces (surfaces), edges (curves) and vertices (points).
- Many different cell/element and grid types are available.
Choice depends on the problem and the solver capabilities.

Grids:

- Structured grid
 - all nodes have the same number of elements around it
 - only for simple domains
- Unstructured grid
 - for all geometries
 - irregular data structure



Structure/unstructured mesh

- Structured grid

Advantages:

- Economical in terms of both memory & computing time
- Easy to code/more efficient solvers available
- The user has full control in grid generation
- Easy in post processing

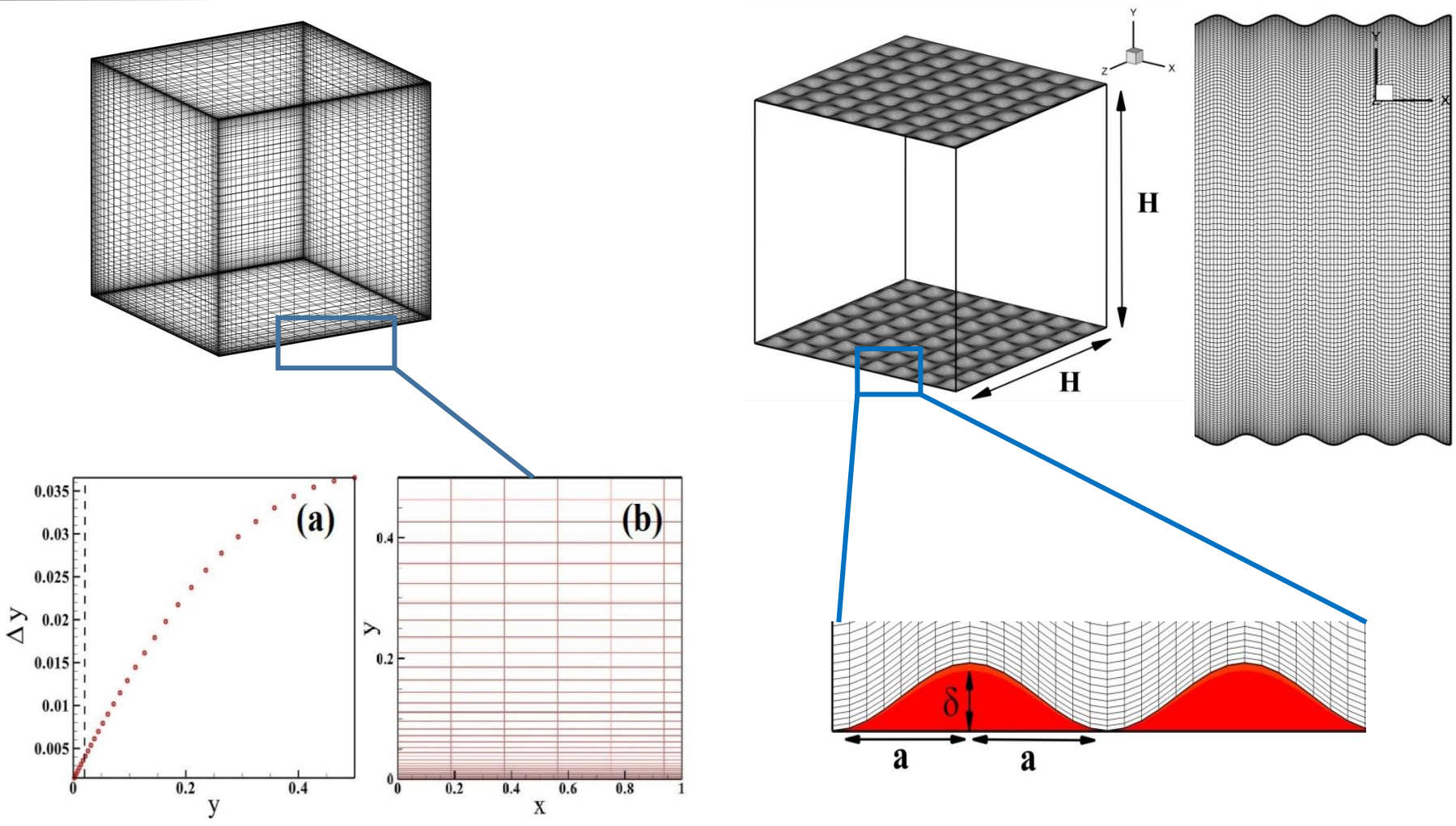
Disadvantages

- Difficult to deal with complex geometries

- Unstructured grid

- Advantages/disadvantages: opposite to above points!!

Structure/unstructured mesh



Stretched grid points within the thermal boundary layer (close to the solid wall)

Errors involved in CFD results

- Discretization errors
 - Depending on ‘schemes’ used. Use of higher order schemes will normally help to reduce such errors
 - Also depending on mesh size – reducing mesh size will normally help to reduce such errors. (skewness)
- Iteration errors
 - For converged solutions, such errors are relatively small.
- Turbulence modelling
 - Some turbulence models are proved to produce good results for certain flows
 - Some models are better than others under certain conditions
 - But no turbulence model can claim to work well for all flows
- Physical problem *vs* mathematical model
 - Approximation in boundary conditions
 - Use of a 2D model to simplify calculation
 - Simplification in the treatment of properties

Introduction

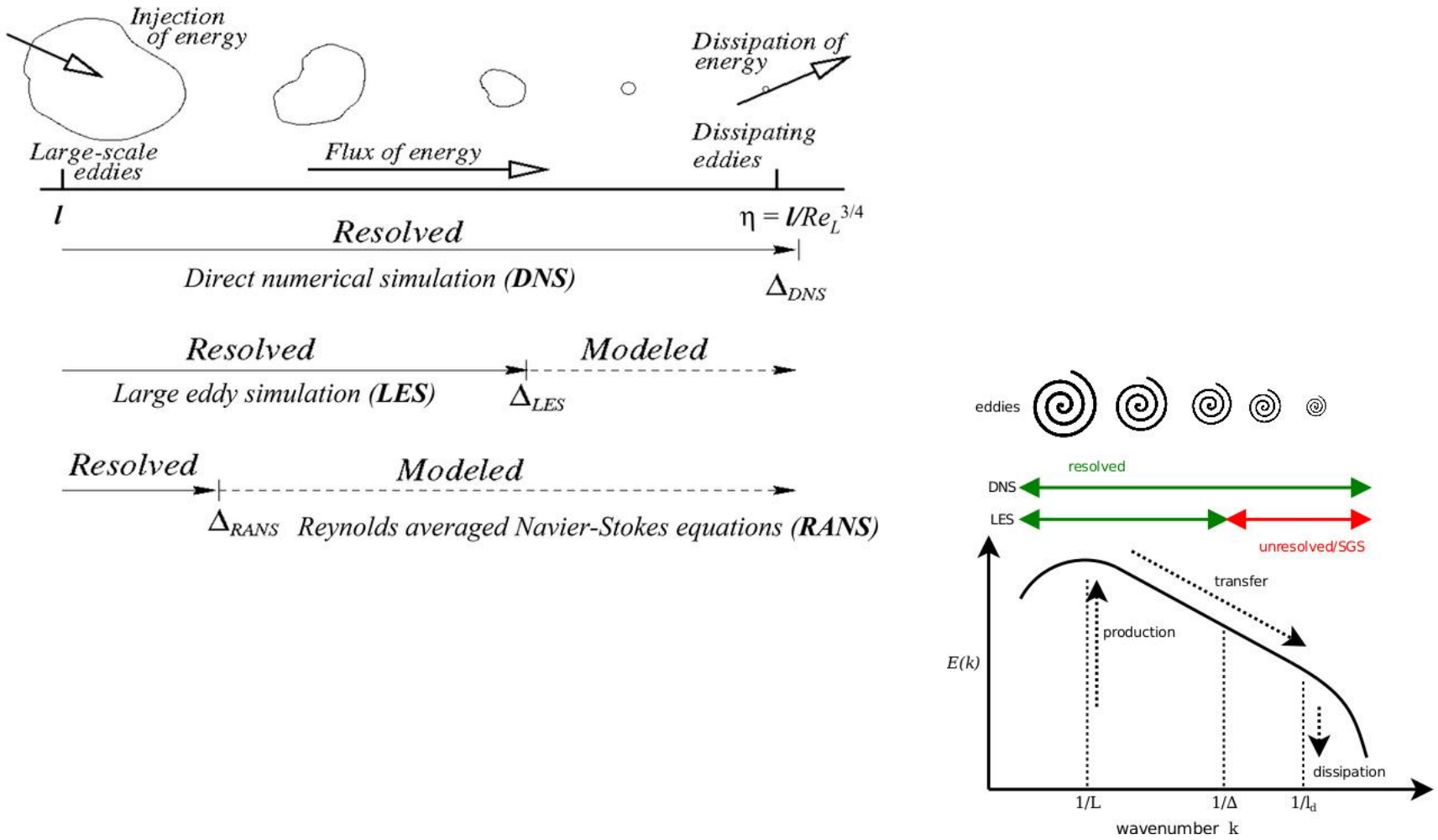
The three levels
of simulations

Reynolds-averaged
modeling (RANS)

Direct Numerical
Simulation
(DNS)

Large Eddy
Simulations
(LES)

Energy cascade



Reynolds-Averaged NS equations (RANS)

A more sophisticated method involves the use of Reynolds averaging: the long term average of a quantity f is defined as

$$\bar{f} = \frac{1}{T} \int_t^{t+T} f(\tau) d\tau$$

where T is a time interval much longer than all the time scales of the turbulent flow.

By averaging the Navier-Stokes equations, we obtain the Reynolds averaged Navier-Stokes (RANS) equations;

$$\frac{\partial u_i}{\partial x_i} = 0, \quad \rho \frac{\partial u_i}{\partial t} + \rho \frac{\partial}{\partial x_j} (u_j u_i) = - \frac{\partial p}{\partial x_i} + \frac{\partial}{x_j} (2\mu S_{ij})$$

$$\frac{\partial \bar{u}_i}{\partial x_i} = 0, \quad \rho \frac{\partial \bar{u}_i}{\partial t} + \rho \frac{\partial}{\partial x_j} (\bar{u}_j \bar{u}_i) = - \frac{\partial \bar{p}}{\partial x_i} + \frac{\partial}{x_j} (2\mu S_{ij} - \rho \bar{u}'_i \bar{u}'_j)$$

$$R_{ij} = -\rho \begin{bmatrix} \overline{u'u'} & \overline{u'v'} & \overline{u'w'} \\ \overline{v'u'} & \overline{v'v'} & \overline{v'w'} \\ \overline{w'u'} & \overline{w'v'} & \overline{w'w'} \end{bmatrix}$$

In order to close the RANS equations, the Reynolds stress tensor must be modeled.



How can we close the RANS equations?

The objective of the turbulence models for the RANS equations is to compute the Reynolds stresses, which can be done by three main categories of RANS-based turbulence models:

- Linear eddy viscosity models
- Nonlinear eddy viscosity models
- Reynolds stress model (RSM)
- Two equation models: k - ε style

Direct Numerical Simulation (DNS)

- **Direct numerical simulation (DNS)** is a simulation in CFD in which the NS-equations are numerically solved **without any** turbulence model. This means that the whole range of spatial and temporal scales of the turbulence must be resolved. All the spatial scales of the turbulence must be resolved in the computational mesh, from the smallest dissipative scales (Kolmogorov microscales), up to the integral scale L , associated with the motions containing most of the kinetic energy.
- ◆ Given the current processing speed and memory of the largest computers, only very modest Reynolds number flows with simple geometries are possible. i.e., The cost of a simulation increases as Re^3
- ◆ **Advantages:** DNS can be used as **numerical flow visualization** and can provide more information than experimental measurements; DNS can be used to understand the mechanisms of turbulent production and dissipation.
- ◆ **Disadvantages:** Requires supercomputers; limited to simple geometries.
- ◆ **Is DNS a useful tool?**

Large Eddy Simulation (LES)

- KEY IDEA is to directly **solve** the unsteady and 3D large-scale energy-carrying structures and to **parametrize** the more isotropic and dissipative small structures (subgrid-scales, SGS)
- Separation of the scales: application of a low-pass **filter** to the NS equations

$$\bar{f}(x) = \int_D f(x') G(x, x') dx'$$

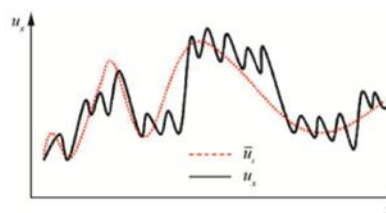
$G(x, x')$ is the filter function

FIRST NEED TO SEPARATE THE FLOW FIELD

Large eddies, most energy and fluxes, explicitly calculated, must be resolved.

Small eddies, little energy and fluxes, parameterized

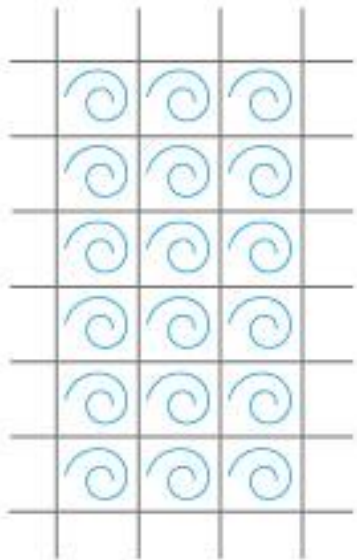
- LES is a three dimensional, time dependent and computationally expensive simulation, though less expensive than DNS.



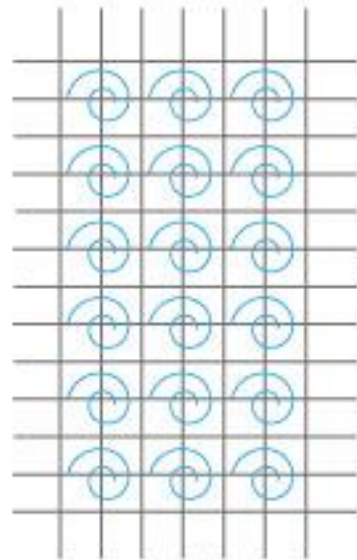


LES vs RANS

- LES **can** handle many flows which RANS (Reynolds Averaged Navier Stokes) **cannot**; the reason is that in LES more, turbulent scales are resolved. Here are some examples that could be studied by LES only:
 - Flows with large separation
 - Bluff-body flows (e.g. flow around a car); the wake often includes large, unsteady, turbulent structures
 - Transition
 - In RANS all turbulent scales are modeled \Rightarrow inaccurate
 - In LES only small, isotropic turbulent scales are modeled \Rightarrow accurate
 - LES is *very* much more expensive than RANS.

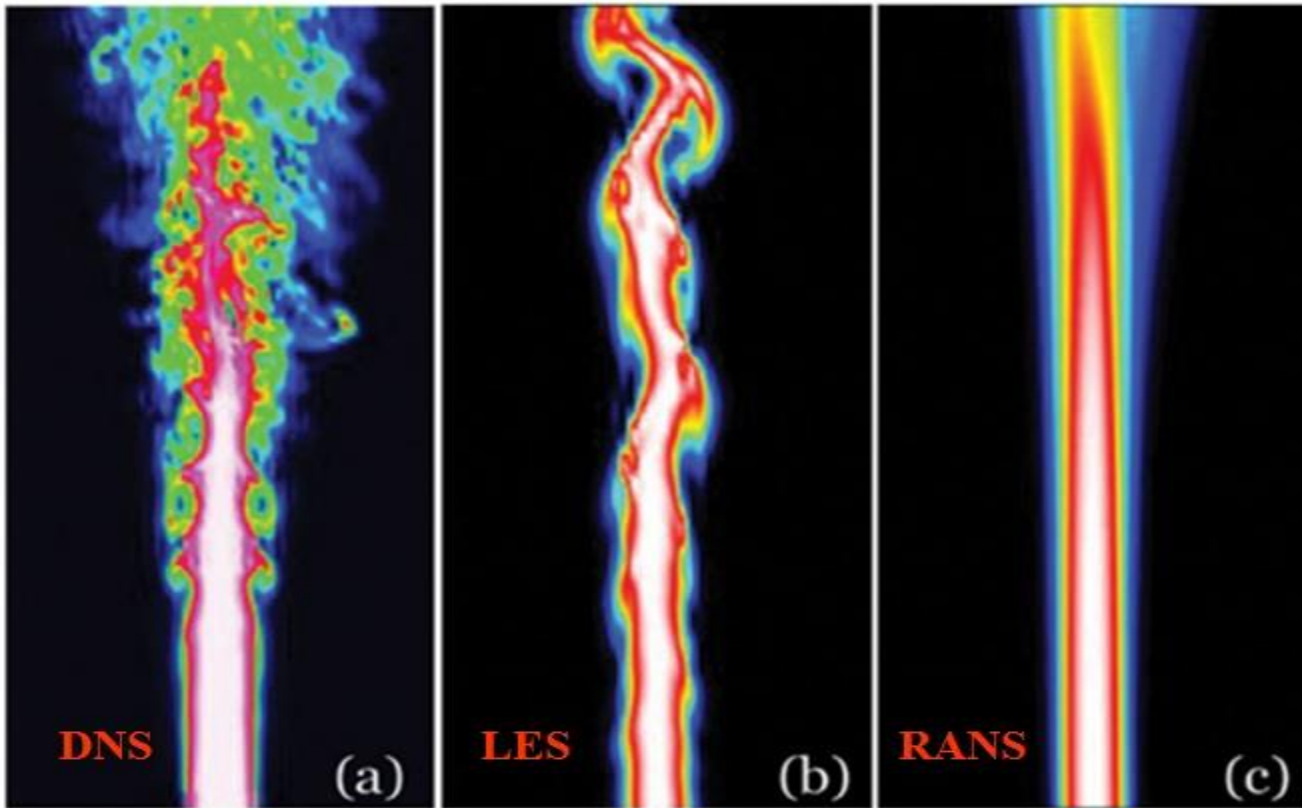


Mesh is coarse for eddies
→ RANS calculation



Mesh is fine for eddies
→ LES calculation

DNS, LES and RANS



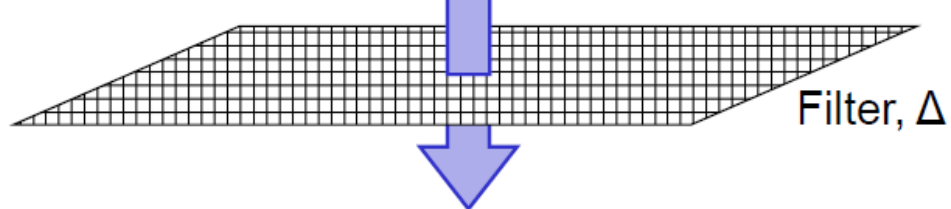
DNS (left), LES (middle) and RANS (right) predictions of a turbulent jet. LES requires less computational effort than DNS, while delivering more detail than the inexpensive RANS. (A. Maries, University of Pittsburgh)

LES

$$u_i(\mathbf{x}, t) = \bar{u}_i(\mathbf{x}, t) + u'_i(\mathbf{x}, t)$$

↑ Instantaneous component ↑ Resolved Scale ↑ Subgrid Scale

$$\frac{\partial u_i}{\partial t} + \frac{\partial (u_i u_j)}{\partial x_j} = -\frac{1}{\rho} \frac{\partial p}{\partial x_i} + \frac{\partial}{\partial x_j} \left(\nu \frac{\partial u_i}{\partial x_j} \right)$$



Filtered N-S
equation

$$\frac{\partial \bar{u}_i}{\partial t} + \frac{\partial (\bar{u}_i \bar{u}_j)}{\partial x_j} = -\frac{1}{\rho} \frac{\partial \bar{p}}{\partial x_i} + \frac{\partial}{\partial x_j} \left(\nu \frac{\partial \bar{u}_i}{\partial x_j} \right) - \frac{\partial \tau_{ij}}{\partial x_j}$$

$$\tau_{ij} = \rho (\bar{u}_i u_j - \bar{u}_i \bar{u}_j)$$

(Subgrid scale Turbulent stress)

- Spectrum of turbulent eddies in the Navier-Stokes equations is filtered:
 - The filter is a function of grid size
 - Eddies smaller than the grid size are removed and modeled by a subgrid scale (SGS) model.
 - Larger eddies are directly solved numerically by the filtered transient NS equation

Filtered momentum equation

- Filter the momentum eq. with an arbitrary homogenous filter of width $\bar{\Delta}$
- homogeneity of filter allows commutation with differentiation:

$$\frac{\partial \bar{u}_i}{\partial t} + \frac{\partial(\bar{u}_i \bar{u}_j)}{\partial x_j} = -\frac{\partial \bar{p}}{\partial x_i} + \frac{1}{\text{Re}} \frac{\partial^2 \bar{u}_i}{\partial x_j^2}$$

- $\bar{u}_i \bar{u}_j = \bar{u}_i \bar{u}_j + \bar{u}_i \bar{u}_j - \bar{u}_i \bar{u}_j$ leads to

$$\frac{\partial \bar{u}_i}{\partial t} + \frac{\partial(\bar{u}_i \bar{u}_j)}{\partial x_j} = -\frac{\partial \bar{p}}{\partial x_i} + \frac{1}{\text{Re}} \frac{\partial^2 \bar{u}_i}{\partial x_j^2} - \frac{\partial \tau_{ij}}{\partial x_j}$$

$$\tau_{ij} = \bar{u}_i \bar{u}_j - \bar{u}_i \bar{u}_j$$

- τ_{ij} is an **unknown** stress accounting for the effect of the filtered-out small scales on the large scales governed by the filtered equation

Residual (subgrid-scale (SGS)) stress

- Note that in general: $A_{ij}^d \equiv A_{ij} - (1/3)\delta_{ij}A_{kk}$

Decompose the SGS stress as

$$\tau_{ij}^d = (\overline{u_i u_j}_2 - \overline{\bar{u}_i \bar{u}_j}_2) - \frac{1}{3} \delta_{ij} (\overline{u_k u_k}_2 - \overline{\bar{u}_k \bar{u}_k}_2)$$

τ_{ij} τ_{kk}

deviatoric (trace-free) component

- This decomposition leads to

$$\frac{\partial \bar{u}_i}{\partial t} + \frac{\partial(\bar{u}_i \bar{u}_j)}{\partial x_j} = -\frac{\partial \bar{P}}{\partial x_i} + \frac{1}{\text{Re}} \frac{\partial^2 \bar{u}_i}{\partial x_j^2} - \frac{\partial \tau_{ij}^d}{\partial x_j}$$

- The modified filtered pressure contains the isotropic part of the SGS stress

Filtered equations

$$\frac{\partial \bar{u}_i}{\partial x_i} = 0$$

SGS stress



$$\frac{\partial \bar{u}_i}{\partial t} + \bar{u}_j \frac{\partial \bar{u}_i}{\partial x_j} = - \frac{\partial \bar{P}}{\partial x_i} + \frac{1}{\text{Re}} \frac{\partial^2 \bar{u}_i}{\partial x_j^2} - \frac{\partial \tau_{ij}^d}{\partial x_j} + Ri(\bar{\rho} - \bar{\rho}_b)$$

$$\frac{\partial \bar{\rho}}{\partial t} + \bar{u}_i \frac{\partial \bar{\rho}}{\partial x_i} = \kappa \frac{\partial^2 \bar{\rho}}{\partial x_i^2} - \frac{\partial \lambda_i}{\partial x_i}$$

SGS density flux

SGS stress: $\tau_{ij}^d = (\overline{u_i u_j} - \bar{u}_i \bar{u}_j)^d \equiv (\overline{u_i u_j} - \bar{u}_i \bar{u}_j) - \frac{1}{3} \delta_{ij} (\overline{u_k u_k} - \bar{u}_k \bar{u}_k)$

SGS density flux: $\lambda_i \equiv \overline{\rho u_i} - \bar{\rho} \bar{u}_i$ (obtained in same way as the SGS stress)

Comments on the filtered equations

- The filtered equations are numerically solved for the filtered $(\bar{u}_i, \bar{\rho}, \bar{P})$ variables describing the large scales
- The SGS stress and SGS density flux present closure problems and must be modeled or approximated in terms of filtered variables only
- In theory, the filter used to obtain the filtered equations is arbitrary
- In practice, the filter is inherently assumed by the discretization (i.e. the numerical method used to solve the filtered equations and the SGS models)
- The discretization can only represent (resolve) down to scales on the order of 1,2, or 3 times the grid cell size, h , thereby “filtering-out” smaller scales.

Smagorinsky SGS model

- Recall that the SGS stress and density buoyancy flux must be modeled or approximated

Smagorinsky (1967) model:

$$\tau_{ij}^d \equiv (\overline{u_i u_j} - \bar{u}_i \bar{u}_j)^d \approx -2\nu_T \bar{S}_{ij}$$

Both are trace-free

$$\nu_T = (C_S \bar{\Delta})^2 |\bar{S}| \quad | \bar{S} | = \sqrt{2\bar{S}_{ij}\bar{S}_{ij}} \quad \bar{S}_{ij} = \frac{1}{2} \left(\frac{\partial \bar{u}_i}{\partial x_j} + \frac{\partial \bar{u}_j}{\partial x_i} \right)$$

Smagorinsky coefficient

Analogously: $\lambda_i \equiv \overline{\rho u_i} - \bar{\rho} \bar{u}_i \approx -\kappa_T (\partial \bar{\rho} / \partial x_i)$

$$\kappa_T = (C_\rho \bar{\Delta})^2 |\bar{S}|$$

The eddy (turbulent) viscosity

The turbulent viscosity has units L^2 / T . Because we are working with the smallest resolved scales, we can set $L = \bar{\Delta}$

- And we may have $T = (\bar{\Delta}^2 / \varepsilon)^{1/3} \Rightarrow \nu_T = C \varepsilon^{1/3} \bar{\Delta}^{4/3}$
- In a global sense, the rate of energy transfer within the inertial range is roughly equal to the **SGS dissipation**. Here we assume it locally:
$$\varepsilon \approx -\tau_{ij}^d \bar{S}_{ij} = \nu_T |\bar{S}|^2 \Rightarrow \nu_T = \underbrace{C_s^{3/2} \bar{\Delta}^2 |\bar{S}|}_{C_s^2}$$

Difficulties with the Smagorinsky model

Smagorinsky model:

$$\tau_{ij}^d \equiv (\overline{u_i u_j} - \bar{u}_i \bar{u}_j)^d \approx -2\nu_T \bar{S}_{ij}$$
$$\nu_T = (C_S \bar{\Delta})^2 |\bar{S}|$$

- For isotropic turbulence, Lilly (1967) showed that $C_S = 0.16$

Major difficulty:

- The constant coefficient allows for a non-vanishing turbulent viscosity at boundaries and in the presence of relaminarization
- The Smagorinsky coefficient should be a function of **space and time**
- In 1991, Germano and collaborators derived a dynamic expression for the Smagorinsky coefficient

Dynamic Smagorinsky model

- Recall filtering the N-S equations with an homogeneous filter of width

$$\frac{\partial \bar{u}_i}{\partial t} + \bar{u}_j \frac{\partial \bar{u}_i}{\partial x_j} = -\frac{\partial \bar{P}}{\partial x_i} + \frac{1}{\text{Re}} \frac{\partial^2 \bar{u}_i}{\partial x_j^2} - \frac{\partial \tau_{ij}^d}{\partial x_j} \quad \tau_{ij}^d \equiv (\bar{u}_i \bar{u}_j - \bar{u}_i \bar{u}_j)^d \approx -2(C_S \bar{\Delta})^2 |\bar{S}| \bar{S}_{ij}$$

Consider a new filter made up from successive applications of the 1st filter (above) and a new “**test**” filter. This “double” filter has width $\hat{\Delta}$

Application of this “double” filter is denoted by a “bar-hat” in the form of \hat{f}

With this new filter, the filtered momentum equation becomes:

$$\frac{\partial \hat{\bar{u}}_i}{\partial t} + \hat{\bar{u}}_j \frac{\partial \hat{\bar{u}}_i}{\partial x_j} = -\frac{\partial \hat{\bar{P}}}{\partial x_i} + \frac{1}{\text{Re}} \frac{\partial^2 \hat{\bar{u}}_i}{\partial x_j^2} - \frac{\partial T_{ij}^d}{\partial x_j} \quad T_{ij}^d \equiv (\bar{u}_i \bar{u}_j - \hat{\bar{u}}_i \hat{\bar{u}}_j)^d \approx -2(C'_S \hat{\Delta})^2 |\hat{\bar{S}}| \hat{\bar{S}}_{ij}$$

- **Scale invariance:** Both $\hat{\Delta}$ and $\bar{\Delta}$ are in the inertial range, thus $C'_S = C_S$

Dynamic Smagorinsky model

- Consider the following tensor proposed by Germano (GI) : $L_{ij}^d \equiv T_{ij}^d - \tau_{ij}^d$

$$L_{ij}^d = (\widehat{\overline{u_i u_j}} - \widehat{\overline{u}_i \overline{u}_j})^d - (\widehat{\overline{u_i u_j}} - \widehat{\overline{u}_i \widehat{\overline{u}}_j})^d = (\widehat{\overline{u_i u_j}} - \widehat{\overline{u}_i \widehat{\overline{u}}_j})^d \quad \leftarrow \text{(resolved)}$$

$$L_{ij}^d = -2(C_S \widehat{\Delta})^2 |\widehat{\overline{S}}| \widehat{\overline{S}}_{ij} + 2(C_S \overline{\Delta})^2 |\widehat{\overline{S}}| \widehat{\overline{S}}_{ij} \quad \leftarrow \text{(modeled)}$$

- Minimization of the difference between these two with respect to C_S leads to:

$$(C_S \overline{\Delta})^2 = \frac{< L_{ij} M_{ij} >}{< 2M_{kl} M_{kl} >}$$

$$M_{ij} = |\widehat{\overline{S}}| \widehat{\overline{S}}_{ij} - \alpha |\widehat{\overline{S}}| \widehat{\overline{S}}_{ij}$$

$< \cdot >$ - Averaging in statistically homogenous direction(s)

$$L_{ij} = \widehat{\overline{u_i u_j}} - \widehat{\overline{u}_i \widehat{\overline{u}}_j} \quad \alpha = \left(\frac{\widehat{\Delta}}{\overline{\Delta}} \right)^2$$

- Explicit application of test filter (denoted by a “hat”) is required, unlike 1st filter

LES methodology used in computations

$$\left\{ \begin{array}{l} \frac{\partial \bar{u}_i}{\partial x_i} = 0 \\ \\ \frac{\partial \bar{u}_i}{\partial t} + \bar{u}_j \frac{\partial \bar{u}_i}{\partial x_j} = -\frac{\partial \bar{P}}{\partial x_i} + \frac{1}{Re} \frac{\partial^2 \bar{u}_i}{\partial x_j^2} - \frac{\partial \tau_{ij}^d}{\partial x_j} + F \delta_{i1} + Ri(\bar{\rho} - \bar{\rho}_b) \\ \\ \frac{\partial \bar{\rho}}{\partial t} + \bar{u}_i \frac{\partial \bar{\rho}}{\partial x_i} = \kappa \frac{\partial^2 \bar{\rho}}{\partial x_i^2} - \frac{\partial \lambda_i}{\partial x_i} \end{array} \right.$$

SGS stress


SGS density flux


SGS stress model:

$$\tau_{ij}^d \approx -2(C_4 \bar{\Delta})^2 | \bar{S} | \bar{S}_{ij}$$

SGS density flux model:

$$\lambda_i \approx -(C_4 \bar{\Delta})^2 | \bar{S} | \frac{\partial \bar{\rho}}{\partial x_i}$$

ν_T
 κ_T

- Model coefficients in SGS models are computed **dynamically** as described

The Dynamic Lagrangian SGS model (Meneveau et al., 1996)

This model tries to improve the performance of the dynamic Smagorinsky model for non-homogeneous flows.

Rationale

- **Dynamic model not reliable without averaging**
 - Numerical instability
- **So some averaging necessary**
 - Global averaging successful but requires homogeneous direction
 - Local averaging possible but results depend on volume chosen
- **Need an averaging procedure that works in complex flows.**

Meneveau *et al.* (1996)* developed a Lagrangian version of DSM where C_s is averaged along fluid-particle trajectories (back in time). The objective function to be minimized is given by

$$E = \int_{pathline} \epsilon_{ij}(z) \epsilon_{ij}(z) dz = \int_{-\infty} \epsilon_{ij}(z(t'), t') \epsilon_{ij}(z(t'), t') W(t - t') dt'$$

Time weighting function: $W(t - t') = T^{-1}e^{-(t-t')/T}$

$$\frac{D\mathfrak{J}_{LM}}{Dt} \equiv \frac{\partial \mathfrak{J}_{LM}}{\partial t} + \bar{u}_i \frac{\partial \mathfrak{J}_{LM}}{\partial x_i} = \frac{1}{T} (L_{ij} M_{ij} - \mathfrak{J}_{LM})$$

$$\frac{D\mathfrak{J}_{MM}}{Dt} \equiv \frac{\partial \mathfrak{J}_{MM}}{\partial t} + \bar{u}_i \frac{\partial \mathfrak{J}_{MM}}{\partial x_i} = \frac{1}{T} (M_{ij} M_{ij} - \mathfrak{J}_{MM})$$

\longrightarrow

$$(C_s \Delta)^2 = \frac{\mathfrak{J}_{LM}}{\mathfrak{J}_{MM}}$$

Time scale $T = \theta \Delta (\mathfrak{J}_{LM} \mathfrak{J}_{MM})^{-1/8}$; $\theta = 1.5$

* SGS density flux computed as (Armenio and Sarkar 2002 JFM):

$$\lambda_j = -C_\rho \Delta^2 |\bar{S}| \frac{\partial \bar{\rho}}{\partial x_j} \quad C_\rho = -\frac{1}{2} \frac{\mathfrak{J}_i \mathcal{M}_i}{\mathcal{M}_k \mathcal{M}_k}$$

$$\mathcal{M}_i = \widehat{\Delta}^2 |\widehat{\bar{S}}| \widehat{\frac{\partial \bar{\rho}}{\partial x_i}} - \widehat{\Delta^2 |\bar{S}| \frac{\partial \bar{\rho}}{\partial x_i}} \quad \mathfrak{J}_i = \widehat{\bar{\rho} \bar{u}_i} - \widehat{\bar{\rho}} \widehat{\bar{u}_i}$$

In summary....

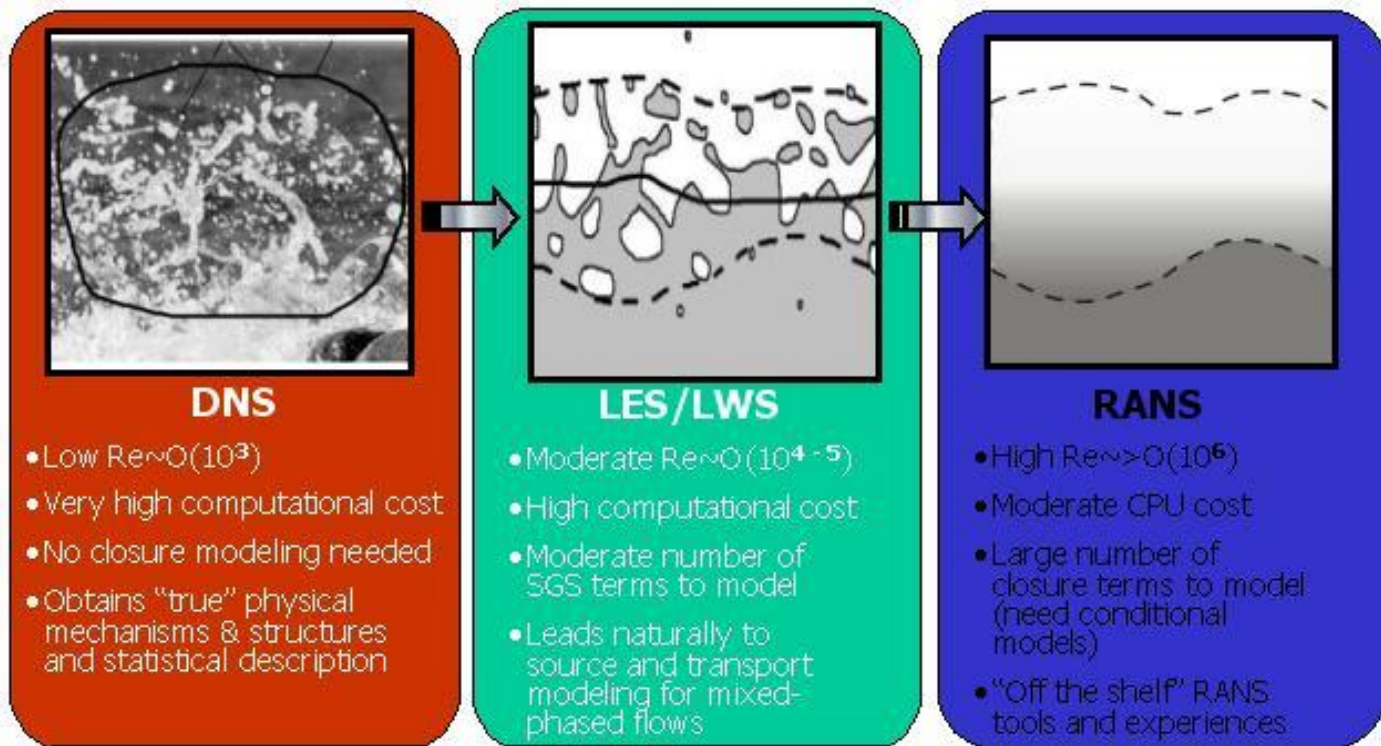
DNS , LES, RANS require solving the unsteady form of the NS or RANS equations.

Main differences between steady-flow and unsteady-flow solvers are:

In steady –flow algorithms, typically continuity equation is not satisfied during the time-advancement of the solution and conservation laws are fulfilled at the convergent state of the solution

In unsteady-flow solvers conservation laws are satisfied at each time step
This makes a strong difference in CPU time request.

Typically projection methods are employed



General remarks on turbulence models

- There are no generically best models.
- Near wall treatment is generally a very important issue.
- A good mesh is important to get good accurate results.
- Different models may have different requirement on the mesh.
- Expertise/validation are of great importance to CFD.

Motivation of the Study

VOLUME 87, NUMBER 18

PHYSICAL REVIEW LETTERS

29 OCTOBER 2001

Does Turbulent Convection Feel the Shape of the Container?

Z. A. Daya and R. E. Ecke

PHYSICAL REVIEW E 90, 063003 (2014)

Influence of container shape on scaling of turbulent fluctuations in convection

N. Foroozani,^{1,2} J. J. Niemela,¹ V. Armenio,² and K. R. Sreenivasan³

Formulation of the problem

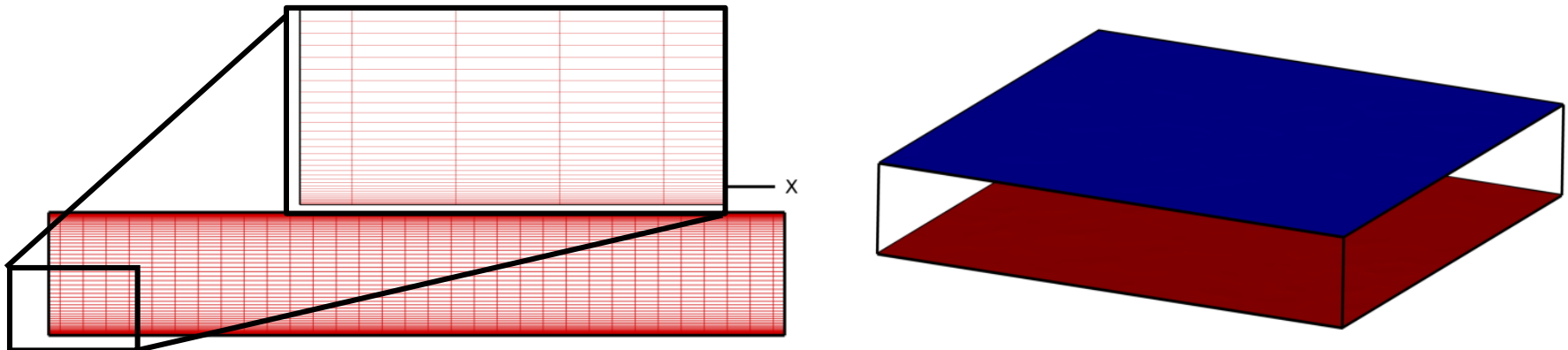
$$\frac{\partial \bar{u}_j}{\partial x_j} = 0,$$

$$\frac{\partial \bar{u}_i}{\partial t} + \frac{\partial \bar{u}_j \bar{u}_i}{\partial x_j} = -\frac{1}{\rho_0} \frac{\partial \bar{P}}{\partial x_i} + \nu \frac{\partial^2 \bar{u}_i}{\partial x_j \partial x_j} - \frac{\bar{\rho}}{\rho_0} g \delta_{i2} - \frac{\partial \tau_{ij}}{\partial x_j},$$

$$\frac{\partial \bar{\rho}}{\partial t} + \frac{\partial \bar{u}_j \bar{\rho}}{\partial x_j} = k \frac{\partial^2 \bar{\rho}}{\partial x_j \partial x_j} - \frac{\partial \lambda_j}{\partial x_j},$$

RBC with periodic walls, but why?

- First we need to find a proper numerical method in terms of definite geometry therefore we performed LES and DNS in an unbounded, homogeneous, domain.
- Our geometry is a 3D rectangular box (6,1,6) ($\Gamma = 6$), note in our study “ y ” is in vertical direction, with periodic boundary conditions over horizontal domain ($x-z$), no-slip velocity on the top and bottom surface, $\frac{d\rho}{\rho_0} = 1$ is applied in wall normal directions
- Molecular Prandtl number $Pr=1$ and Ra number vary $6.3 \times 10^5 \leq Ra \leq 10^8$.
- The vertical resolution in all LES was chosen such that the thermal boundary layer λ_θ is properly resolved.



Introduction

The number of nodes required in thermal and viscous boundary layers computed as:

$$\begin{cases} \frac{\lambda_\theta}{H} = \frac{1}{2Nu} \\ \frac{\lambda_u}{H} \sim \frac{1}{4\sqrt{RaPr}} \end{cases}$$

$$\begin{cases} N_\theta \approx 0.35Ra^{0.15} & 10^6 \leq Ra \leq 10^{10} \\ N_u \approx 0.13Ra^{0.15}, & 10^6 \leq Ra \leq 10^{10} \end{cases}$$

Shishkina *et al.*, 2010.

We performed two tests for LES:

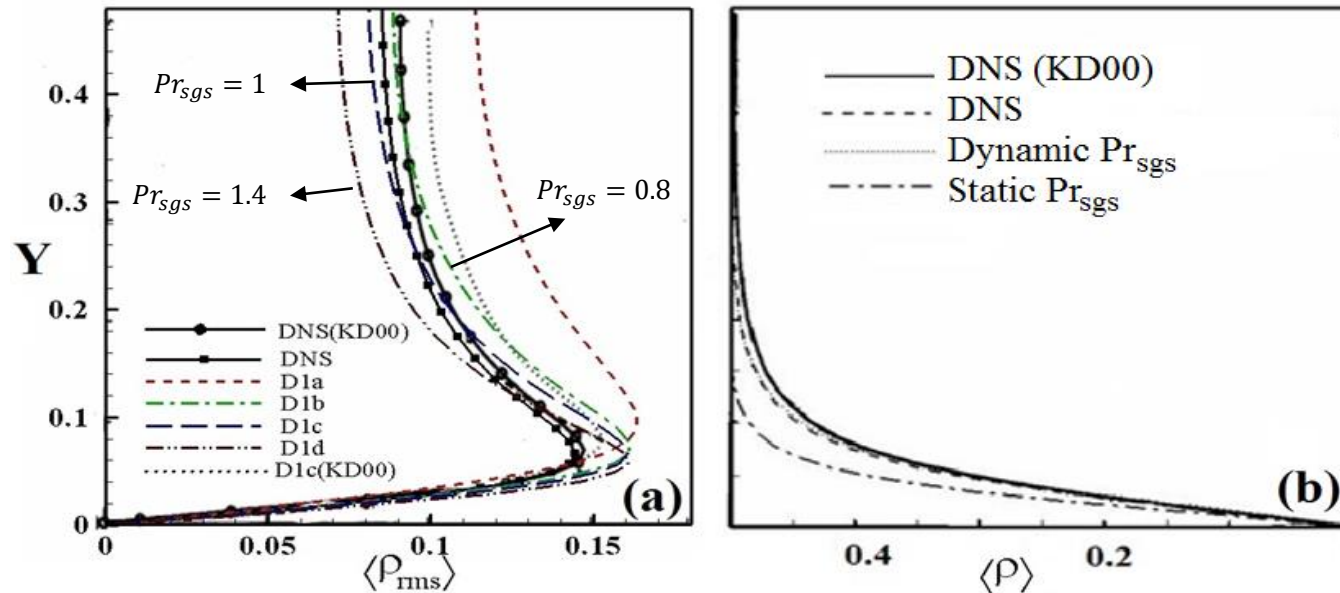
- 1) $\kappa_{sgs} = \frac{v_{sgs}}{Pr_{sgs}}$ with Pr_{sgs} set *a priori* test (static)
- 2) **Both** v_{sgs} and κ_{sgs} calculated dynamically

Introduction

$$\text{Total turbulent fluctuations} = \underline{\text{Resolved}} + \underline{\text{SGS}}$$

The resolved root-mean-square of density fluctuations computed as:

$$\rho_{rms} = [\langle \rho(x)\rho(x) \rangle_t - \langle \rho(x) \rangle_t \langle \rho(x) \rangle_t]^{1/2}$$



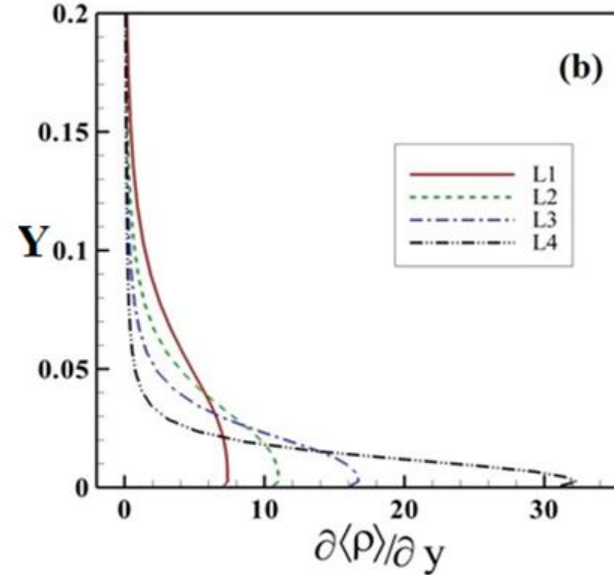
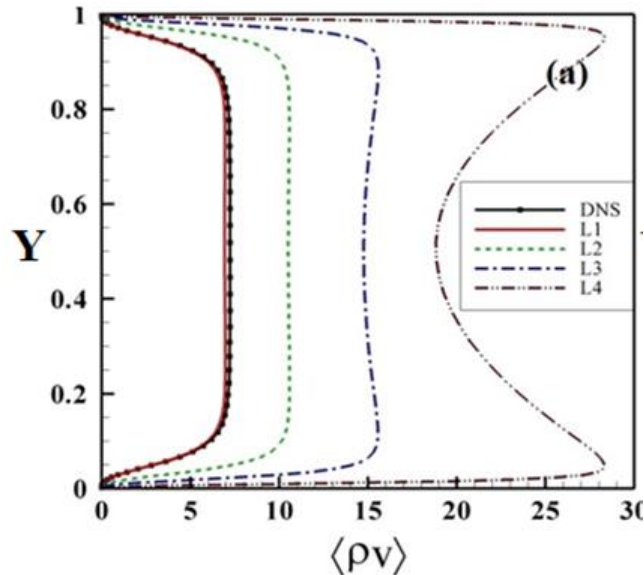
- (a) The resolved rms density fluctuations computed with the dynamic model at $Ra = 6.3 \times 10^5$ on the $32 \times 64 \times 32$ grids (b) Mean density profiles for $Ra = 6.3 \times 10^5$ with dynamic (L0) and static (D1c) Pr_{sgs} . Data are compared with Kimmel and Domaradzki (2000).

Introduction

The key response of the system to the imposed parameters is the heat flux from bottom to top (Nu).

Global Nusselt number:

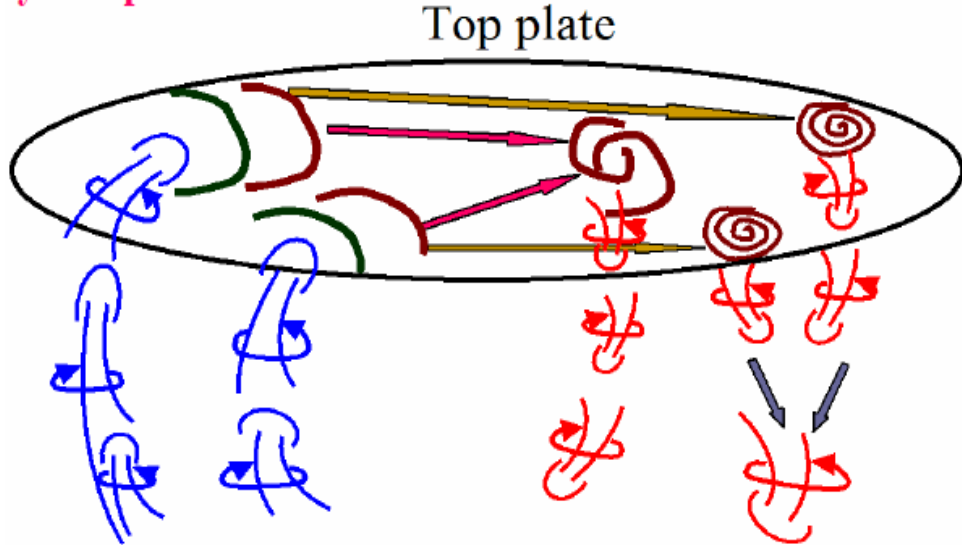
$$Nu = \frac{\langle \rho v \rangle_{A,t} - \kappa \frac{\partial \langle \rho \rangle_{A,t}}{\partial y}}{\kappa \Delta \gamma / H} \rightarrow Nu = 0.14 Ra^{0.29}$$



Comparison of the Nusselt number , Nu, components using dynamic Pr_{sgs} as a function of Ra numbers; (a) resolved vertical density flux and (b) resolved density gradient along vertical direction. The letters represent L1 (6.3×10^5), L2 (2.5×10^6), L3 (10^7), L4 (10^8)

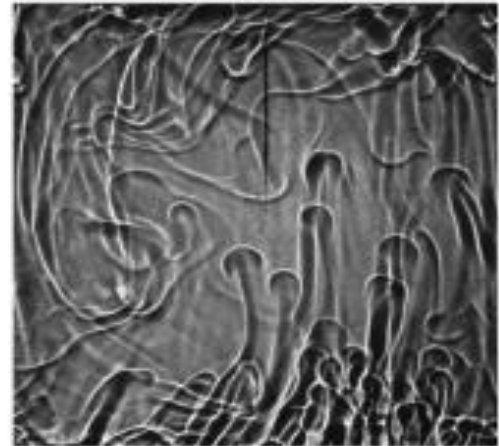
Flow topology in convection

Physical picture



- Sheetlike plume
- Convoluted sheetlike plume

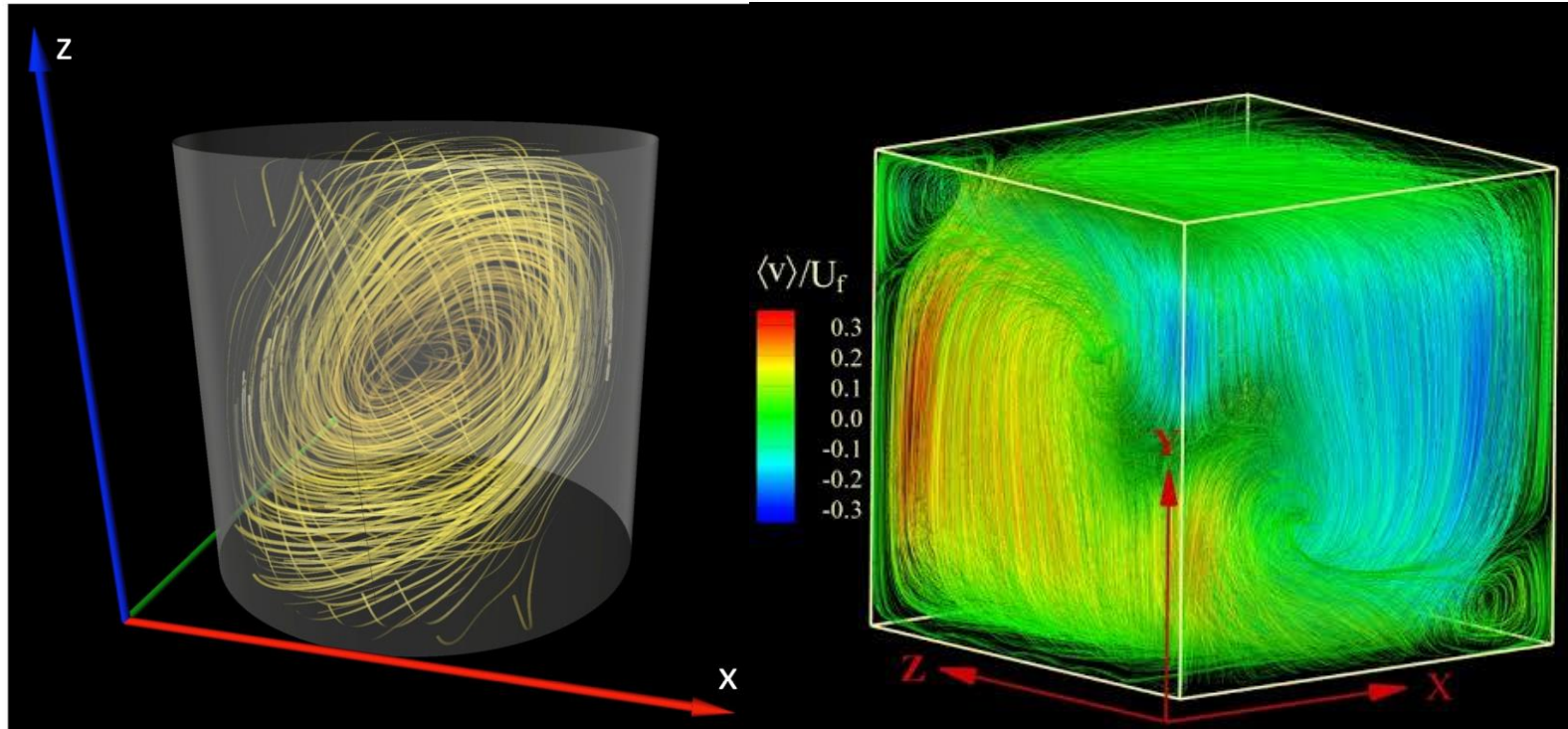
- Mushroomlike plume with strong vertical vorticity



Mushroom-like plumes (side view)

Zhang et al, PoF 2007

The mean wind

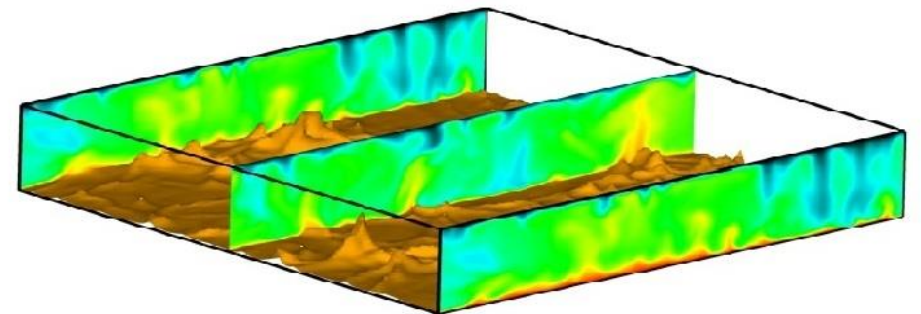


For convection in a round cylinder, the mean wind precesses freely.

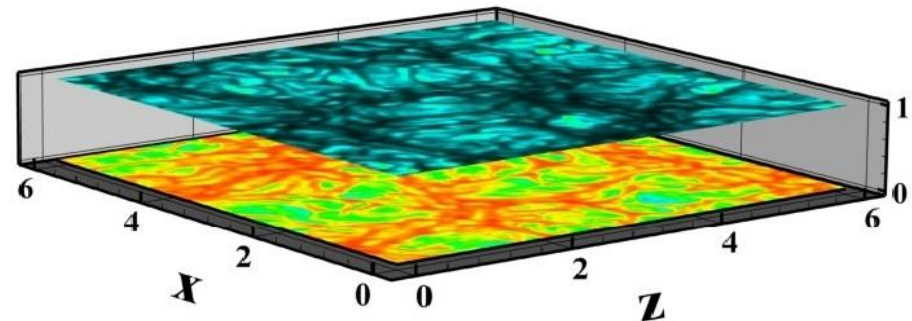
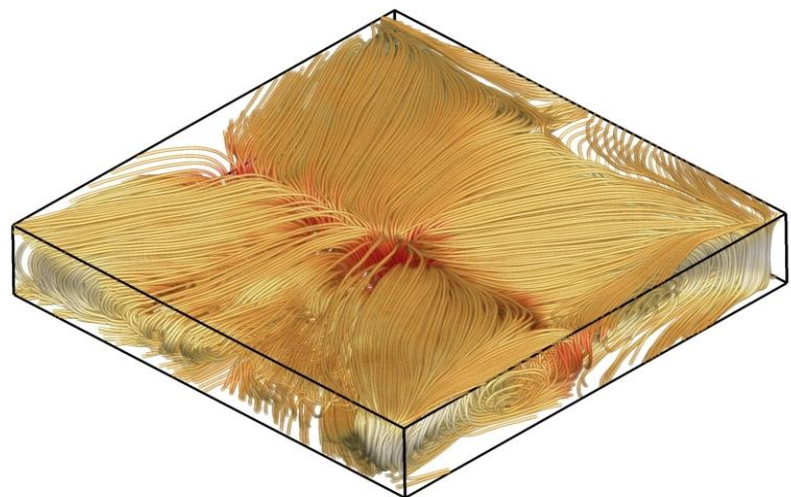
For convection in a cubic box, the mean wind is constrained along a diagonal.

From my simulation...

Instantaneous field



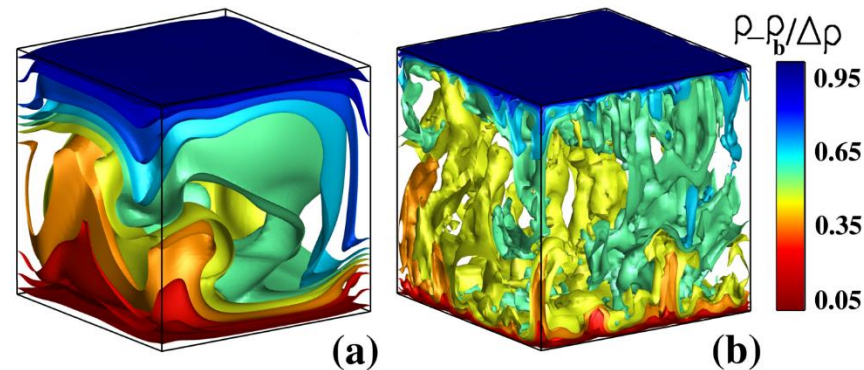
Time averaged field



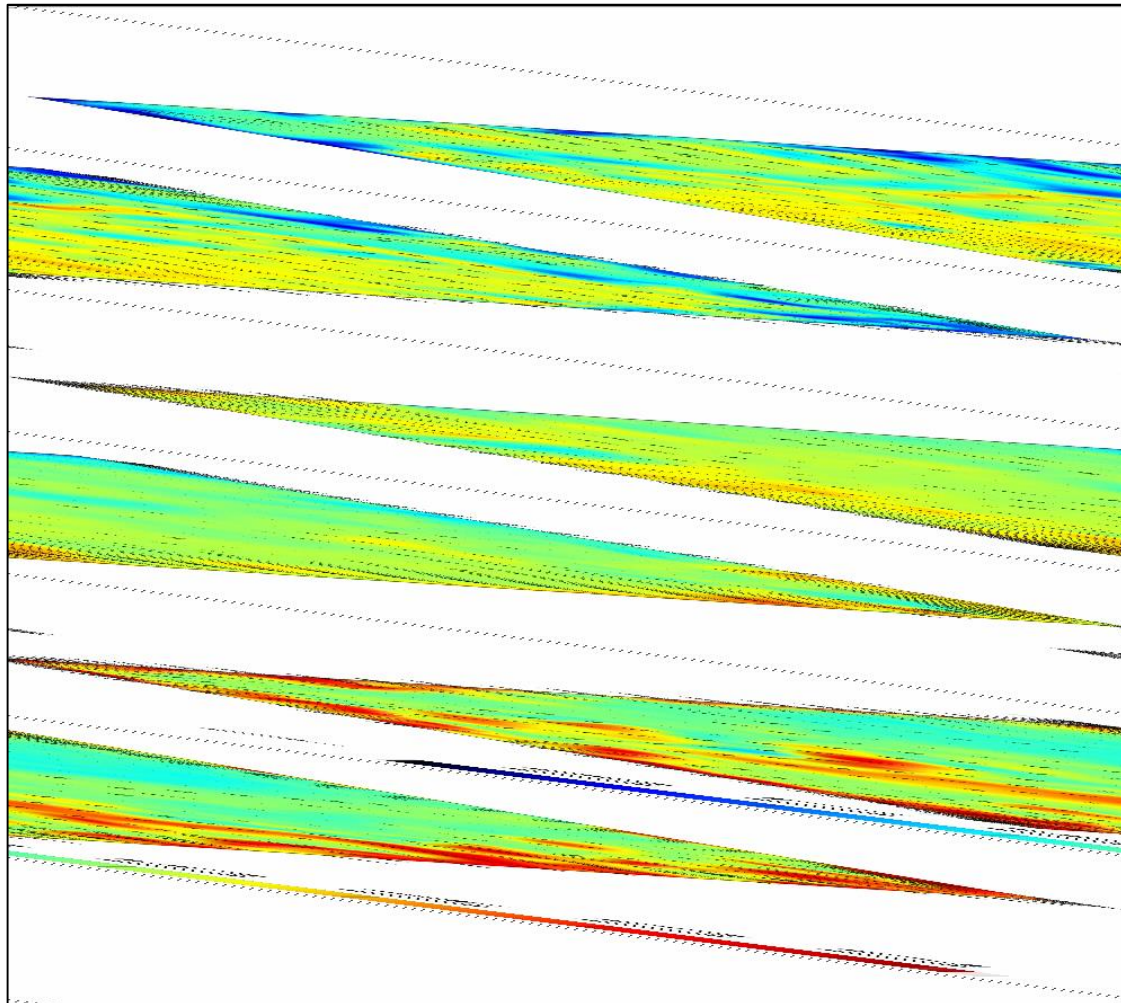
Influence of the geometry

- We perform LES in a **closed** cubic cell $\Gamma=1$, for $10^6 < Ra < 10^{10}$, molecular Prandtl number set to $Pr = 0.7$
 - Vertical walls are adiabatic ($\partial\rho/\partial\vec{n}=0$),
 - We applied no-slip BCs at the walls,
 - Finer grid close to the walls (Verzicco and Camussi JFM 2003),
 - We use coarse grid at low Ra numbers, and finer resolution at high Ra. Hyperbolic tangent function is used to stretch the mesh.
- ✓ We compute global Nusselt number:
- $$Nu = \frac{\kappa \partial_y \langle \rho \rangle_{A,t} - \langle u_y \rho \rangle_{A,t}}{\kappa \Delta \rho H^{-1}}$$
- ✓ Scaling of Nu(Ra) is in good agreement with both the laboratory experiment [Qiu & Xia 1998], and DNS of Kaczorowski & Xia 2013 (JFM 722,569)

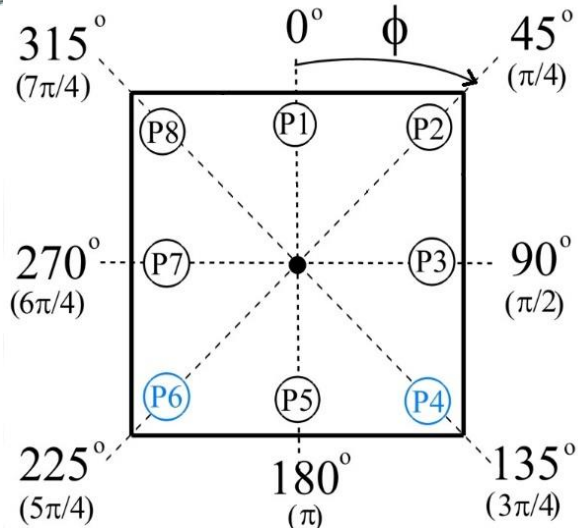
Ra	$N_x \times N_y \times N_z$	N_{BL}	Nu	Nu_{Ref}
1×10^6	$32 \times 64 \times 32$	14	8.31	8.32
3×10^6	$32 \times 64 \times 32$	11	11.4	11.5
1×10^7	$32 \times 64 \times 32$	10	16.4	16.3
3×10^7	$32 \times 64 \times 32$	8	22.4	22.0
1×10^8	$32 \times 64 \times 32$	6	31.6	31.3
1×10^9	$64 \times 96 \times 64$	5	63.4	
1×10^{10}	$64 \times 96 \times 64$	5	116.2	



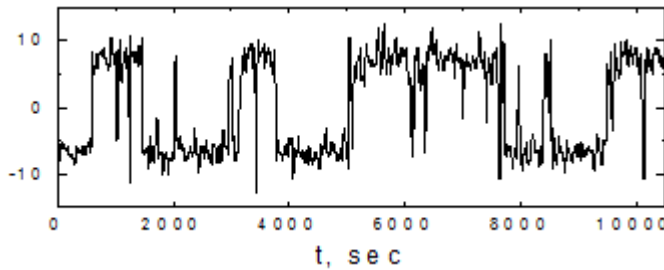
Structures of the mean flow



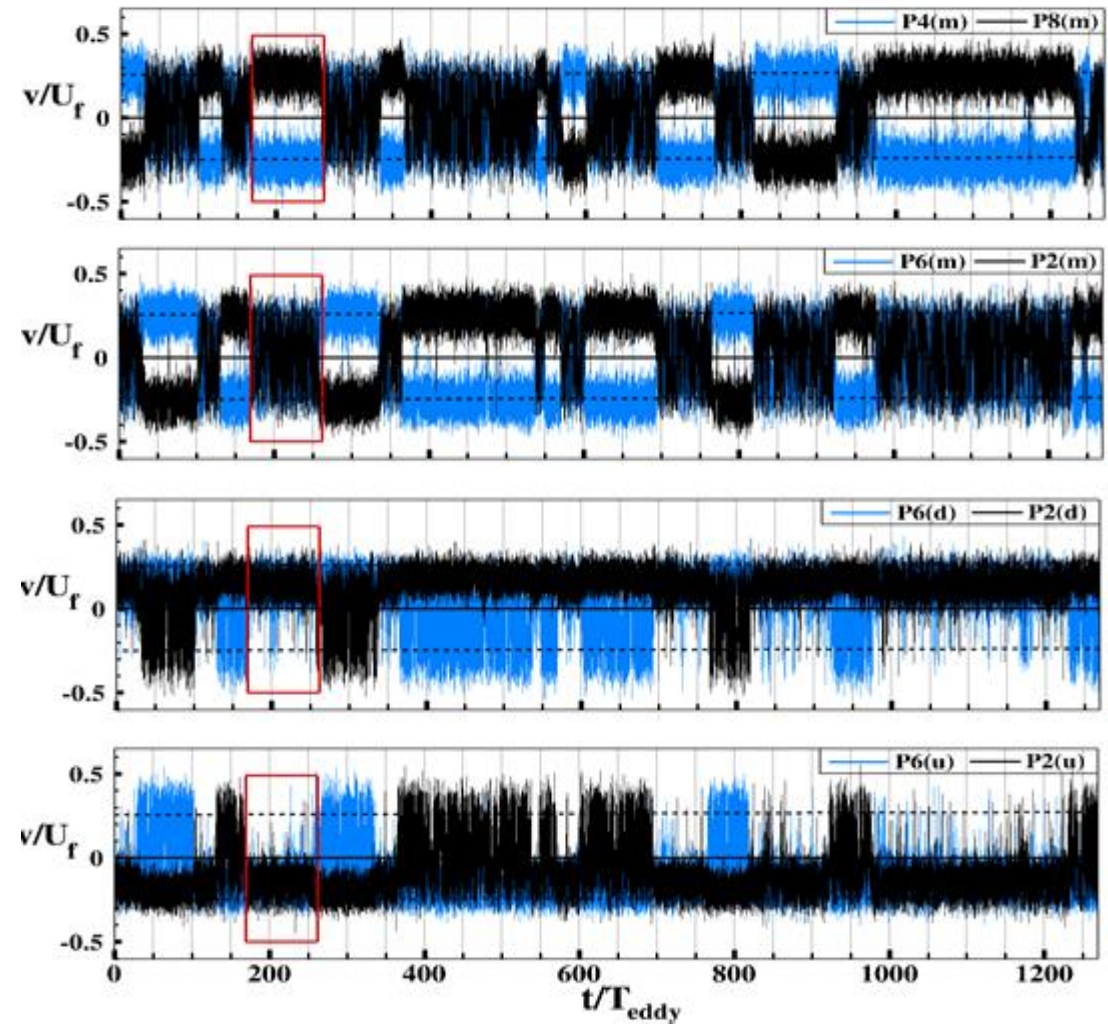
Velocity statistics



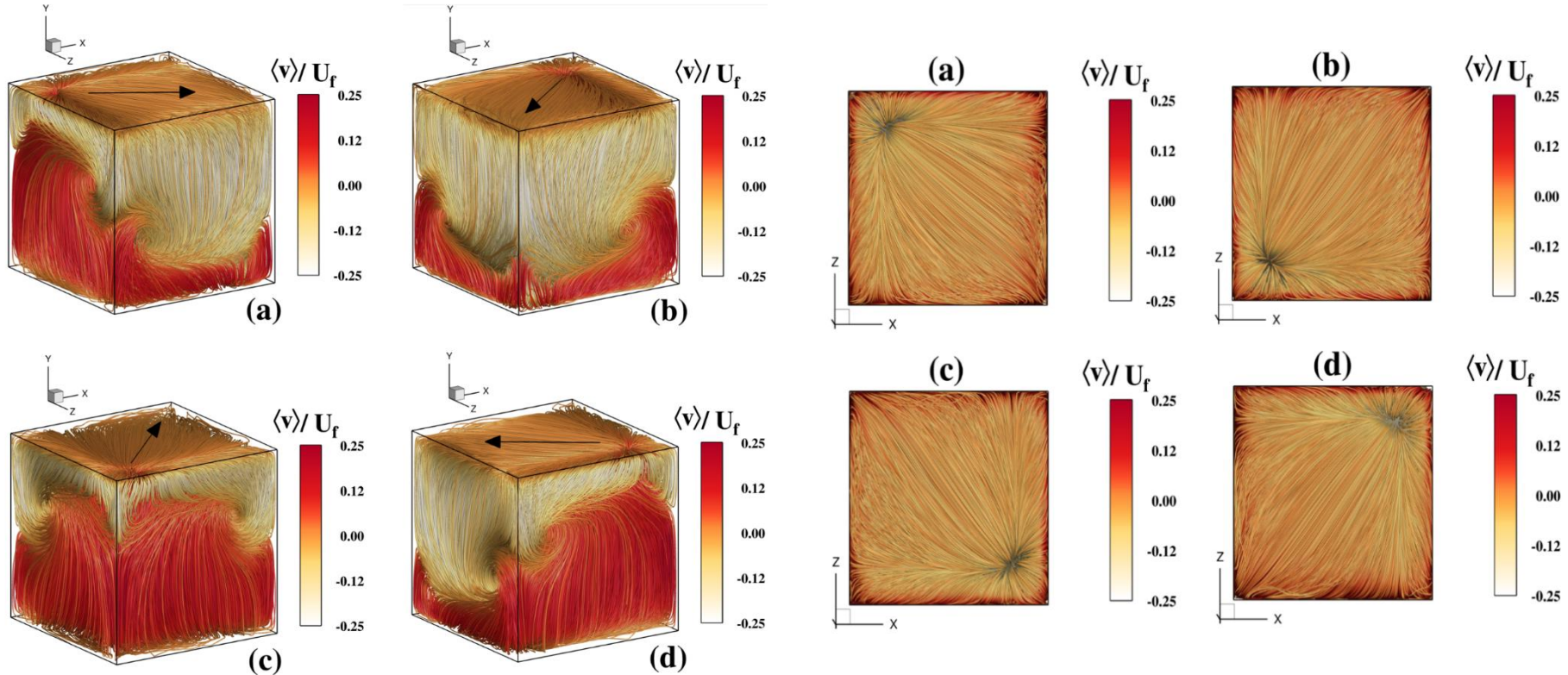
Schematic of an arbitrary horizontal plane showing the azimuthal positions for probes, placed at azimuthal angles $\varphi_i = (i\pi)/4$, $i=1,\dots,8$. The distance from the vertical walls are 0.1H for all cases.



Niemela and Sreenivasan, *Nature* (2000).

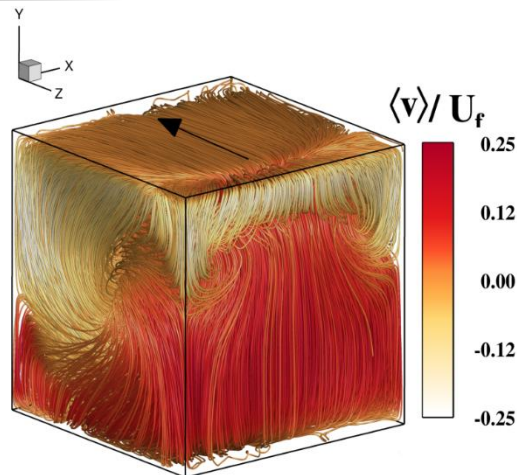


Mean flow structure at $Ra = 10^8$



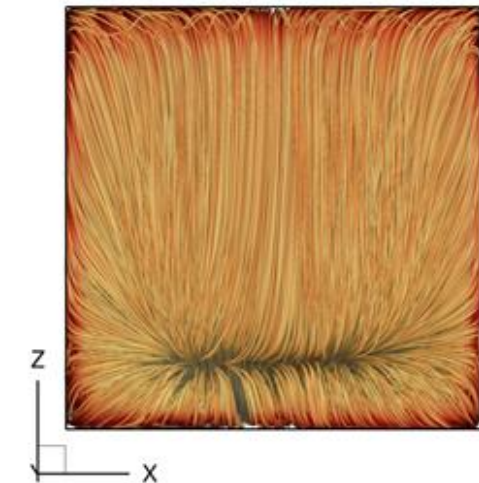
Time averaged of velocity streamlines. The color coding depicts the magnitude of the vertical velocity normalized by free fall velocity. The large arrow shows the direction of the LSC.

Transient state during the re-orientation of the LSC

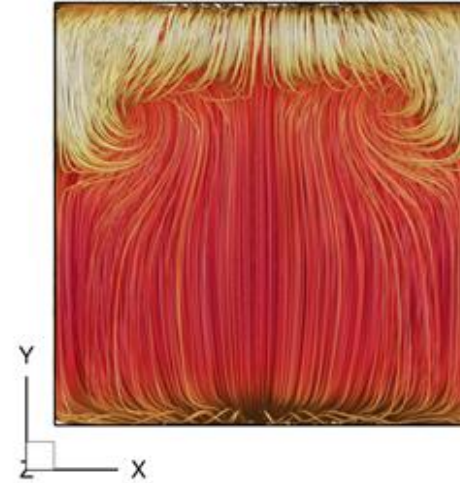


The 3D perspective of the transition state of the global ow structure during a reorientation of the LSC from one stable diagonal plane to the other.

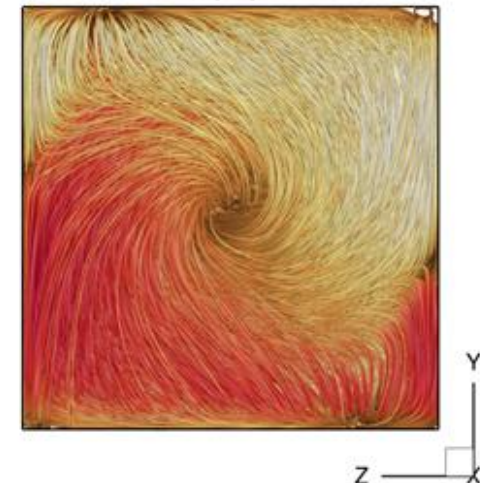
(a)



(b)



(c)



Thermal Convection in the presence of rough surfaces

